

Design and Implementation of Modified Sliding Mode Controller for a Photovoltaic System

Venkata Ratnam Kolluru¹, Kamalakanta Mahapatra², Bidyadhar Subudhi³

¹Department of ECE, NIT-Rourkela, Odisha, India, venkataratnamk@gmail.com

²Department of ECE, NIT-Rourkela, Odisha, India, kkm@nitrkl.ac.in

³Department of EE, NIT-Rourkela, Odisha, India, bidyadhar@nitrkl.ac.in

Abstract— This paper gives an idea about Sliding Mode Controller (SMC) implementation to a DC-DC Boost Converter for a Photovoltaic (PV) system to track Maximum Power Point (MPP). SMC implementation meets three steps (i) Hitting condition, (ii) Existence condition and (iii) Stability condition. Single diode PV model is designed for lighting applications, and PV output is connected to a Boost converter to regulate and increase the voltage upto desired level. SMC is implemented in a feedback manner with capacitor voltage and inductor current. The steady state condition occurred very quickly i.e., before 0.1sec, and the results of SMC are compared with PI controller. The models are simulated in MATLAB/SIMULINK.

Index Terms— DC DC Boost Converter, Maximum Power Point (MPP), Photovoltaic(PV), Sliding Mode Controller (SMC).

I. INTRODUCTION

Solar power has exceptional potential as a renewable energy generation source due to the abundance of solar power and the resulting pollution free generation of direct current. The PV power generation is based on the principle of the photovoltaic effect [1]. With the advent of silicon p-n junctions, the photoelectric current is able to produce power [2] due to inherent voltage drop across the junction. However, such power generation is well-known for the nonlinear relationship between the current and voltage of the photovoltaic cell. It is observed that, there is a unique point at which the photovoltaic cell produces maximum power. At this point, the rate of change of power with respect to the voltage is equal to zero. The advancements in the area of power electronics have made photovoltaic technology much more efficient and cost-effective.

There are several power management issues concerning improvement in the conversion efficiency of a PV array, thus maximizing PV power output. PV array has to be operated at MPP in order to extract maximum power output. The maximum power of the PV array changes with shading and/or climatic conditions [3]. The PV output current/voltage changes with solar irradiation levels, whereas the PV output voltage changes with temperature of the PV array. Thus, an important challenge in a PV system [4] is to ensure that maximum energy is generated from the PV array with a dynamic variation of its output characteristic when connected to a variable load. A solution for this problem is the insertion of a power converter between the PV array and load, which

could dynamically change the impedance of the circuit by using a control algorithm. DC DC Converters are required to regulate the output voltage[5] at a required level. In this paper, DC DC Boost (step up)converter is used, that has a capability of providing an output voltage which is higher than the input voltage.

The new SMC approach is recognized as one of the efficient and robust controller for non linear plants operating under varying conditions [6] - [10]. Here, in order to approach the SMC, mathematical modeling of SMC should meet the conditions like hitting, SM existence and stability, which are part of sliding mode control theory [6]. SMC is to employ a certain sliding surface as a reference path [11] such that the trajectory of the controlled system is directed to the desired equilibrium point. The frequency oscillations may occur in the control process which is reflected in the actual behavior of the trajectory [12], called as chattering. The trajectory ‘S’ chatters along the surface and move towards the origin.

Section II of this article presents a mathematical modeling of a PV cell explanation. Section III is devoted for a DC DC boost converter with state space analysis. Section IV is dedicated to design and implementation of modified SMC for a boost converter. Section V summarizes the comparison and discussion on simulation results (SMC with PI) and finally conclusion ends the paper in Section VI.

II. MODELLING OF A PV DEVICE

PV is one of the methods of renewable energy generations, which means generating electrical power by converting solar irradiation into direct current. Now, PV is one of the popular renewable energy generation sources due to the availability of solar energy and resulting emanation of free generation. The basic diagram of a PV cell is shown in Fig. 1. When the solar irradiation falls on photovoltaic material, it converts into direct current. The current source is connected in parallel to a diode, the current through the diode D is I_d and the diode is connected in a reverse direction to regulate the voltage of a PV cell.

Two resistors are connected (in series and in parallel) to the current source. Generally R_{sh} (parallelly connected resistor) is very high and R_s (series connected resistor) is almost equal to zero, so, the maximum current will flow to the output side. A series resistor R_s , which determines the downward slope of I-V curve in PV cell near V_{oc} , represents

the internal resistance of the cell. A shunt resistor R_{sh} , which determines the slope of the line at a top of I-V curve nearer to I_{sc} [4], controls the leakage current from cell to ground, and is usually small enough to be neglected. The diode current equation expressed[2] is as follows:

$$I_d = I_0 [e^{qV_d/nkT} - 1] \quad (1)$$

where, q = charge of the electron ($1.6 \times 10^{-19} C/ol$), V_d = Diode voltage, k = Boltzman's constant ($1.3 \times 10^{-23} J/K$), T =Absolute temperature, n =Ideality factor, I_0 =Saturation current.

Apply Kirchoff's Current Law (K.C.L) in the PV cell, then the mathematical equation [1] (if R_{sh} is not considered) is

$$I_{ph} - I_d = I_L \quad (2)$$

Substitute (1) in (2)

$$I_{ph} - I_0 [e^{qV_d/nkT} - 1] = I_L \quad (3)$$

After solving (3), which can be expressed in terms of voltage is expressed in the following equation:

$$V_L = \frac{nkT}{q} \ln \left(\frac{I_{ph} - I_L}{I_0} + 1 \right) - I_L R_s \quad (4)$$

From (4), the open circuit voltage (V_{oc}) can be expressed as

$$V_{oc} = \frac{nkT}{q} \ln \left(\frac{I_{ph}}{I_0} + 1 \right) \quad (5)$$

Final expression of the PV cell drawn in Fig. 1 is computed and shown below:

$$V_L = \frac{nkT}{q} \left[\ln \left(\frac{I_{ph} - I_L}{I_0} + 1 \right) - \frac{V_L + I_L R_s}{R_{sh}} \right] - I_L R_s \quad (6)$$

After mathematical modeling of a PV cell is done, we simulated it in MATLAB/SIMULINK and obtained the I-V and P-V characteristic curves at standard test conditions. The waveforms are shown in Fig. 2 and Fig. 3

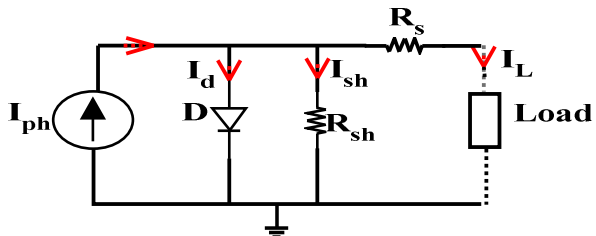


Fig. 1. Circuit of a PV cell single diode model

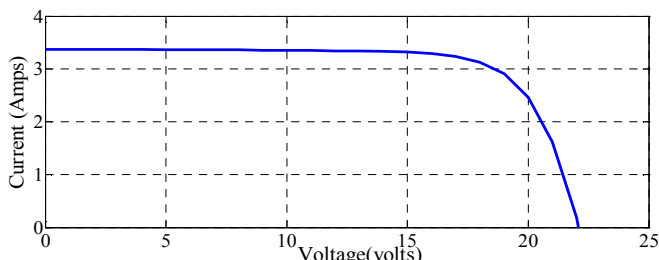


Fig. 2. PV array I-V characteristic curve

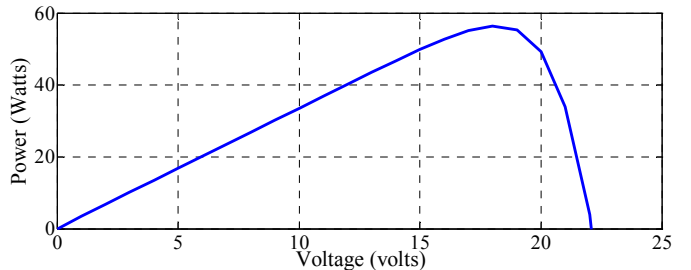


Fig. 3. PV array P-V characteristic curve

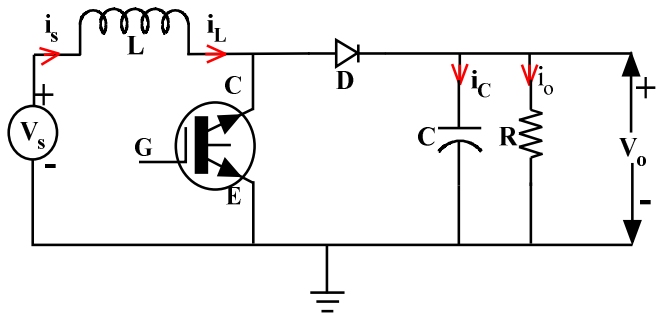


Fig. 4. Circuit of a Boost converter

III. CONTROLLER BASED DC DC BOOST CONVERTER

The DC DC boost converter is a power electronics device also called as a step up converter has a capability of providing the output voltage higher than the input voltage [5], [12]. The circuit diagram of a boost converter is shown in Fig. 4. In boost converter an inductor is connected in series with a supply voltage V_s and a transistor connected for switching across the inductor and supply. A filter capacitor is connected across the load to make the output smooth; the diode 'D' blocks the reverse flow of current when the switch is turned ON. The equivalent circuit diagram of the boost converter when the transistor is 'ON' is shown in Fig. 5.

When the transistor is turned ON, the current flows from the supply to the inductor L , and at this condition the diode 'D' is reverse biased and it does not conduct. Hence the inductor stores the current, then inductor current rises, and the capacitor 'C' maintains the voltage ' V_o ' and supplies current ' i_o '. The mathematical model of a boost converter when the transistor is ON can be expressed in state space[5] as follows:

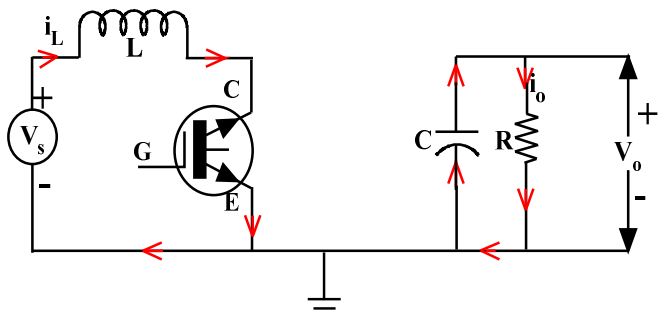


Fig. 5. Equivalent circuit when the transistor is ON

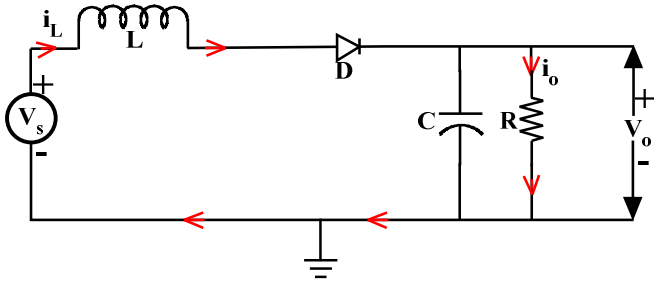


Fig. 6. Equivalent circuit when the transistor is OFF

$$\begin{bmatrix} \frac{dI_L}{dt} \\ \frac{dV_o}{dt} \end{bmatrix} = \begin{bmatrix} 0 & 0 \\ 0 & -\frac{1}{CR} \end{bmatrix} \begin{bmatrix} I_L \\ V_o \end{bmatrix} + \begin{bmatrix} \frac{1}{L} \\ 0 \end{bmatrix} V_s \quad (7)$$

$$V_o = \begin{bmatrix} 0 & -\frac{1}{CR} \end{bmatrix} \begin{bmatrix} I_L \\ V_o \end{bmatrix} \quad (8)$$

When the transistor is turned OFF, the inductor generates a large voltage to maintain the current i_L in the same direction and now the diode D is forward biased and it starts conducting. The equivalent circuit diagram of boost converter when transistor gets OFF, is shown in Fig. 6. Hence the output voltage can be expressed as

$$V_o = V_s + L \frac{di_L}{dt} \quad (9)$$

Thus the output voltage of the converter is higher than the supply voltage V_s , also called as step-up operation. The voltage induced in the inductor adds to the supply voltage and this total voltage appears as output voltage; at that situation the capacitor C also charges to the boosted voltage. The inductor and supply voltage provides energy to the load when the transistor is turned OFF. Current through the inductor decreases because its stored energy goes on reducing. After some time the transistor is again turned ON and the cycle repeats. The mathematical model of a boost converter when the transistor is OFF can be simply expressed in state space as

$$\begin{bmatrix} \frac{dI_L}{dt} \\ \frac{dV_o}{dt} \end{bmatrix} = \begin{bmatrix} 0 & -\frac{1}{L} \\ \frac{1}{C} & -\frac{1}{CR} \end{bmatrix} \begin{bmatrix} I_L \\ V_o \end{bmatrix} + \begin{bmatrix} I_L \\ 0 \end{bmatrix} [V_s] \quad (10)$$

$$V_o = \begin{bmatrix} \frac{1}{C} & -\frac{1}{CR} \end{bmatrix} \begin{bmatrix} I_L \\ V_o \end{bmatrix} \quad (11)$$

IV. SLIDING MODE CONTROLLER FOR BOOST CONVERTER

The MPPT with SMC for boost converter is a method which alleviates the deteriorations that commences an additional integral control variable into the constant frequency SM controller [13]. The involvement of SMC is to enhance the robustness and regulation of the system[14]. Therefore, the

aforementioned uses, mulling over the control performance and simplicity of implementation, adopting an SMC is a better option. SMC introduces a linear combination of a system states, which has the same order of the converter [15].

The fundamental principle of an SMC is to design a particular sliding manifold in its control law that will preside over the trajectory of the state variables towards the required operating point. In case of a boost converter as it has a single switch, it is apt to adopt a control law for a switching function [6] as

$$u = \frac{1}{2}(1 + \text{sgn}(S)) \quad (12)$$

where, u = switching logic of converter, 'S' is an instantaneous state trajectory.

In this case, 'S' is illustrated as

$$S = \alpha_1 x_1 + \alpha_2 x_2 + \alpha_3 x_3 = J^T x \quad (13)$$

with $J^T = [\alpha_1 \ \alpha_2 \ \alpha_3]$ and $\alpha_1, \alpha_2, \alpha_3$ representing the control parameters also considered as sliding coefficients, x_1, x_2, x_3 are the desired state feedback variables which are to be controlled. By equating $S=0$, a sliding plane can be acquired. The aim of the designer is to determine the state of switching function 'u' and also to chose appropriate values of α_1, α_2 and α_3 such that the controller satisfies the hitting, SM existence and stability conditions [6].

A. Hitting condition

The design of SMC to meet the hitting condition is straight forward in the case of power converters. Now the state variables can be expressed in the form of

$$\begin{bmatrix} x_1 \\ x_2 \\ x_3 \end{bmatrix} = \begin{bmatrix} V_{ref} - \beta V_o \\ \frac{d(V_{ref} - \beta V_o)}{dt} \\ \int (V_{ref} - \beta V_o) dt \end{bmatrix} \quad (14)$$

In order to design the hitting condition, it is sufficient to depend only on the immediate state variable x_1 , which is predominant during the reaching phase of 'S'. The resulting control function in this configuration is

$$u = \begin{cases} 1 = ON, & \text{When } S > 0 \\ 0 = OFF, & \text{When } S < 0 \end{cases} \quad (15)$$

Thus, the method ensures fulfillment of hitting condition of the SMC, which is nearly related to the way in which the hysteresis controller switching states are designed.

B. SM Existence condition

With the switching states of the converter determined, the next step is to select the sliding coefficients α_1, α_2 and α_3 that fulfills the condition for SM existence. Now, by inspecting a local reachability condition of the state trajectory, i.e.,

$$\lim_{s \rightarrow 0} S \cdot \dot{S} < 0 \quad (16)$$

$$\dot{S} = J^T \dot{x} \quad (17)$$

$$\dot{x} = Ax + Bu + D \quad (18)$$

Now, this can be expressed as

$$\begin{cases} \dot{S} \\ \dot{S} \end{cases}_{\substack{s \rightarrow 0^+}} = J^T A_x + J^T B v_{s \rightarrow 0^+} + J^T D < 0 \quad (19)$$

$$\begin{cases} \dot{S} \\ \dot{S} \end{cases}_{\substack{s \rightarrow 0^-}} = J^T A_x + J^T B v_{s \rightarrow 0^-} + J^T D < 0$$

Case 1: $S \rightarrow 0^+, \dot{S} < 0$

Substitution of $v_{s \rightarrow 0^+} = \bar{u} = 0$ gives

$$-\alpha_1 \frac{\beta i_c}{C} + \alpha_2 \frac{\beta i_c}{r_L C^2} + \alpha_3 (V_{ref} - \beta V_o) < 0 \quad (20)$$

Case 2: $S \rightarrow 0^-, \dot{S} > 0$

Substitution of $v_{s \rightarrow 0^-} = \bar{u} = 1$ gives

$$\begin{aligned} -\alpha_1 \frac{\beta i_c}{C} + \alpha_2 \frac{\beta i_c}{r_L C^2} + \alpha_3 (V_{ref} - \beta V_o) - \alpha_2 \frac{\beta V_i}{LC} + \\ \alpha_2 \frac{\beta V_o}{LC} > 0 \end{aligned} \quad (21)$$

Finally, the combination of the above two equations gives the simplified existence condition as follows

$$0 < \beta L \left(\frac{\alpha_1}{\alpha_2} - \frac{1}{r_L C} \right) i_C - LC \frac{\alpha_3}{\alpha_2} (V_{ref} - \beta V_o) \quad (22)$$

$$< \beta (V_o - V_i)$$

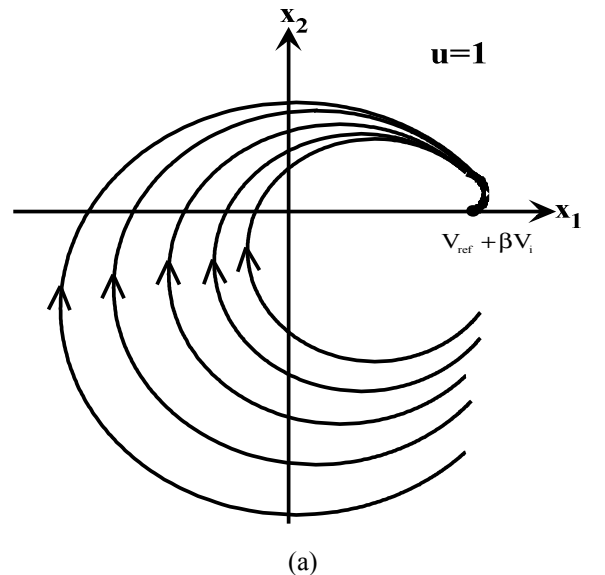
The assortment of sliding coefficients (α_1, α_2 and α_3) for the controller of the boost converter must obey to its stated inequalities. It is important to make sure that the circuit tolerances and operating range of conditions are taken into consideration when evaluating the stated inequalities. This confirms the fulfillment of the SM existence condition for the full operating range of the converters.

C. Stability Condition

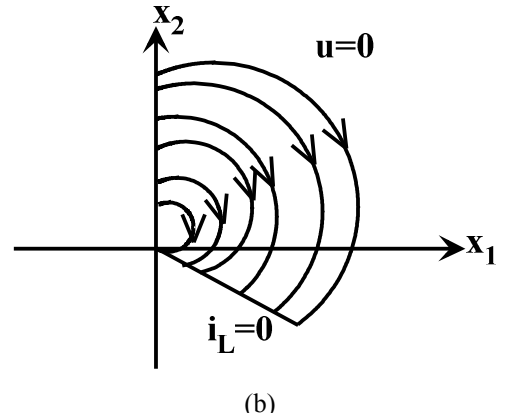
The selected sliding coefficients (α_1, α_2 and α_3) should satisfy the stability condition simultaneously, apart from the fulfillment of SM existence condition. The relation between the sliding coefficients to the dynamic response of the converter during SM operation is

$$\alpha_1 x_1 + \alpha_2 \frac{dx_1}{dt} + \alpha_3 \int x_1 dt = 0 \quad (23)$$

The above equation can be rearranged into standard second order system form in which the design of the sliding coefficients (α_1, α_2 and α_3) will give one of the three possible types of responses like under damped, critical damped and over



(a)



(b)

Fig. 7. Phase trajectories of the substructures at (a) $u=1$, (b) $u=0$ for different starting positions of x_1 and x_2 .

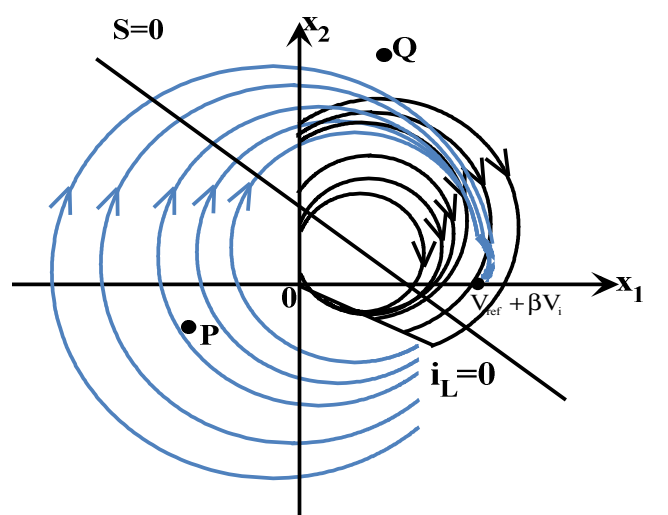


Fig. 8. Combined plot of phase trajectories of the substructures corresponding to $u=1$ and $u=0$ for different starting positions of x_1 and x_2 .

damped. Therefore, selection of sliding coefficients can be easily done by converter response time and voltage peak over shoot specifications.

For an SM voltage controller the switching logical function ‘u’ is obtained by the combination of control parameters[15] x_1 , x_2 and x_3 by utilizing the computation of state trajectories.

$$S = \alpha_1 x_1 + \alpha_2 x_2 + \alpha_3 x_3 = J^T x \quad (24)$$

where α_1 , α_2 and α_3 are considered as control parameters.

By imposing $S=0$, a sliding line is obtained. The main aim of using sliding line is to serve as a periphery to split the phase trajectory, which reaches and tracks the sliding line affirming a system is stable. From Fig. 8, it can be observed that the phase trajectory is at any arbitrary position below the sliding line ($S=0$) e.g., point ‘P’, $u=1$ is employed such that the trajectory is directed towards the sliding line. Similarly, when the trajectories above the sliding line e.g., point ‘Q’, $u=0$ is employed for the trajectory to be directed towards the sliding line.

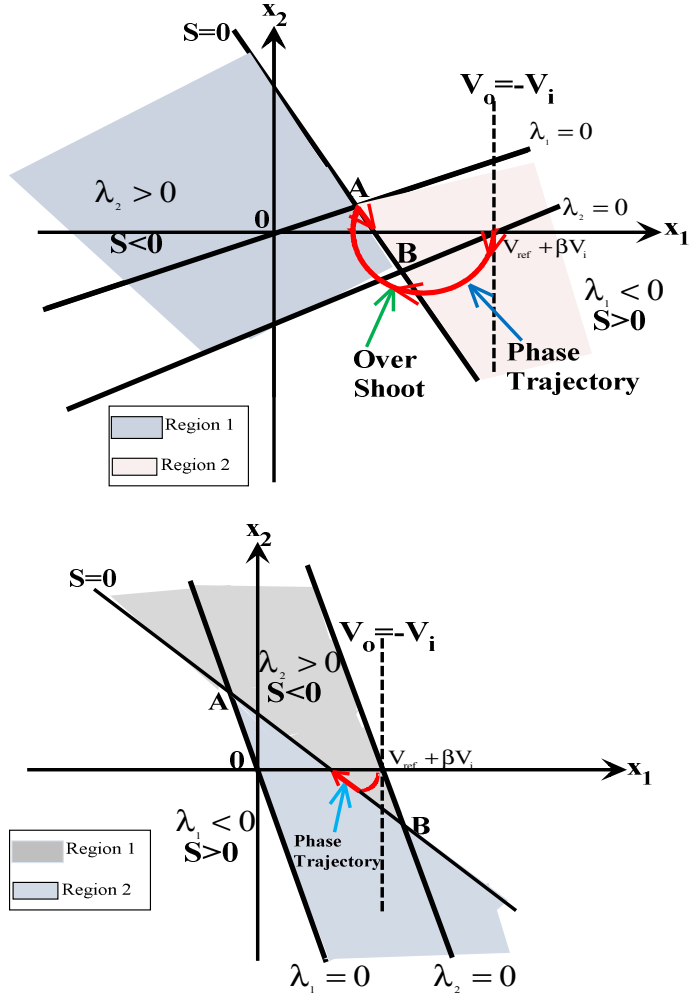


Fig. 9. Regions of SM existence in phase plane a) $\frac{\alpha_1}{\alpha_2} > \frac{1}{R_L C}$, $\frac{\alpha_3}{\alpha_2} < \frac{-1}{LC}$ and b) $\frac{\alpha_1}{\alpha_2} < \frac{1}{R_L C}$, $\frac{\alpha_3}{\alpha_2} < \frac{-1}{LC}$

$$\lambda_1 = (LC \frac{\alpha_3}{\alpha_2} + 1)x_1 + LC(\frac{\alpha_1}{\alpha_2} - \frac{1}{LC})x_2 < 0 \quad (25)$$

$$\lambda_2 = (LC \frac{\alpha_3}{\alpha_2} + 1)x_1 + LC(\frac{\alpha_1}{\alpha_2} - \frac{1}{R_L C})x_2 - (V_{ref} + \beta V_{in}) > 0 \quad (26)$$

The aforementioned conditions are shown in Fig. 9., for the two situations a) $\frac{\alpha_1}{\alpha_2} > \frac{1}{R_L C}$, $\frac{\alpha_3}{\alpha_2} < \frac{-1}{LC}$ and b) $\frac{\alpha_1}{\alpha_2} < \frac{1}{R_L C}$, $\frac{\alpha_3}{\alpha_2} < \frac{-1}{LC}$. In both figures, region 1 depicts $\lambda_1 < 0$ and region 2 represents $\lambda_2 > 0$. The SM operation is only valid on the portion of the sliding line $S=0$, that covers both regions 1 and 2. In this case the portion is within A and B, where A is intersection of $S=0$ and $\lambda_1 = 0$, and B is the intersection of $S=0$ and $\lambda_2 = 0$. Trajectory touches the sliding line $S=0$ within AB, and slides thorough it. When trajectory goes beyond sliding line outside AB, it results an overshoot, when $\frac{\alpha_1}{\alpha_2} > \frac{1}{R_L C}$, $\frac{\alpha_3}{\alpha_2} < \frac{-1}{LC}$.

V. COMPARISON AND DISCUSSION

A proportional-integral (PI) controller is a generic control loop feedback mechanism, widely used in industrial control systems. It calculates an "error" value as the difference between a measured process variable and a desired set point or reference point. Here the voltage outputs of SMC and PI controllers are presented and verified that, the SMC reached steady state condition very quickly (almost 0.06s) than PI controller. Implementation results of the PI and SMC in MATLAB/ SIMULINK is shown in Fig. 10 and the electrical parameters of PV array are listed in Table I.

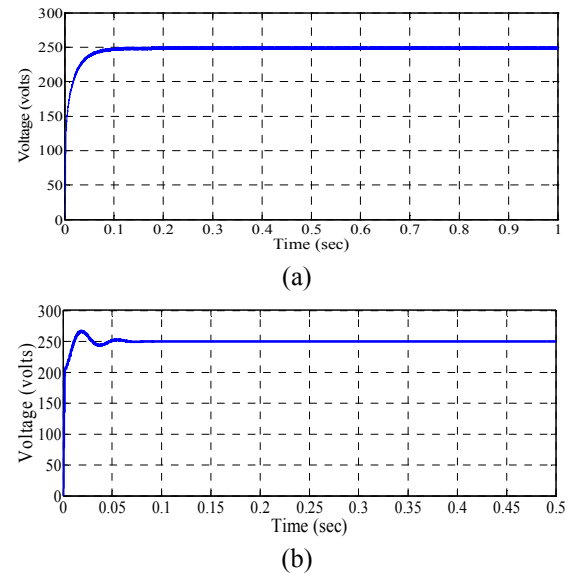


Fig. 10. (a) Voltage output of PI controller, (b) Voltage output of SM controller.

TABLE I
ELECTRICAL PARAMETERS OF PV ARRAY

Maximum power (P_{max})	56W
Voltage at MPP (V_{MPP})	18V
Current at MPP (I_{MPP})	3.13A
Open circuit voltage (V_{oc})	21.9V
Short circuit current (I_{sc})	3.46A

VI. CONCLUSION

In this paper, modified SMC for boost converter is implemented with three basic steps which are (i) Hitting condition (ii) Existence condition and (iii) Stability condition. The modified SMC tracks PV voltage swiftly and reaches steady state condition at 0.06s. The Voltage output of SMC is compared with a PI controller and observed that SMC is almost 40% faster than PI. Phase trajectories at different conditions and SM existence conditions were plotted. Mathematical modeling of a PV cell is analyzed and the output of PV array is connected to a DC DC boost converter for voltage regulation. State space analysis of a boost converter is derived and eventually a boost converter based SMC is developed. With this modified SMC, the reference voltage level and steady state conditions occurred quickly and the results were compared with that of a PI controller.

REFERENCES

- [1] M.G.Villalva, J.R.Gazoli, and E.R.Filho, "Comprehensive approach to modeling and simulation of photovoltaic arrays," *IEEE Trans. Power Electron.*, vol. 24, no. 5, pp. 1198-1208, May 2009.
- [2] R.J.Wai, W.H.Wang, and C.Y.Lin, "High performance stand alone photovoltaic generation system," *IEEE Trans. Ind. Electron.*, vol. 55, no. 1, pp. 240-250, Jan. 2008.
- [3] B.Subudhi, R.Pradhan, "A comparative study on maximum power point tracking techniques for photovoltaic power systems," *IEEE Trans. Sustain. Energy*, vol. 4, no. 1, pp. 89-98, Jan. 2013.
- [4] K.Bouzidi, M.Chegar, and A.Bouhemadou, "Solar cells parameters evalutaion considering the series and shunt resistance," *Sol. Energy Mater. Sol. Cells*, vol. 91, no. 18, pp. 1647-1651, Nov. 2007.
- [5] V.R.Kolluru, K.K.Mahapatra and B.Subudhi "Development and implementation of control algorithms for a photovoltaic system," *IEEE conf. SCES*, Jun. 2013.
- [6] S.C.Tan, Y.Lai and C.Tse, *Sliding Mode Control of Switching Power Converters Techniques and implementation*, 1st ed. Boca Raton, FL: CRC, 2012.
- [7] S.C.Tan, Y.Lai and C.Tse "General desing issues of sliding mode controllers in dc-dc converters," *IEEE Trans. Ind. Electron.*, vol. 55, no. 3, pp. 1160-1174. Mar. 2008.
- [8] S.C.Tan, Y.M.Lai, C.K.Tse, L.M.Salamero and C.K.Wu "A fast response sliding mode controller for boost type converters with wide range of operating conditions," *IEEE Trans. Ind. Electron.*, vol. 54, no. 6, pp. 3276-3286, Dec. 2007.
- [9] J.Knight and S.Shirsavar and W.Holderbaum "An improved reliability cuk based solar inverter with sliding mode control," *IEEE Trans. Power Elect.*, vol. 21, no. 4, pp. 1107-1115, Jul. 2006.
- [10] Y.Levron and D.Shmilovitz "Maximum power point tracking employing sliding mode control," *IEEE Trans. Circuits Syst. I, Reg. Papers*, vol. 60, no. 3, pp. 724-732, Mar. 2013.
- [11] H.Li and X.Ye "Sliding mode PID control of dc-dc converter," *IEEE Int. Conf.*, pp.730-734, 2010.
- [12] H.Guldemir "Sliding mode control of dc-dc boost converter" *Journal of Appl. Sci.*, vol. 5, no. 3, pp. 588-592, 2005.
- [13] Y.P.Jiao and F.L.Luo "An improved sliding mode controller for boost cinverter in solar energy system," *IEEE Int. Conf. ICIEA*, pp. 805-810, 2009.
- [14] J.F.Tsai and Y.P.Chen "Sliding mode control and stability analysis of buck dc-dc converter," *Int. Journal of Elect.*, vol. 94, no. 3, pp. 209-222, Mar. 2007.
- [15] F.Inthamoussou, H.D.Battista and M.Cendoya "Low cost sliding mode power controller of a stand alone photovoltaic module," *IEEE Int. Conf. ICIT*, pp. 1175-1180, 2010.